

Oriented and Nanostructured Polycarbonate Substrates for the Orientation of Conjugated Molecular Materials and Gold Nanoparticles

Martin Brinkmann,^{*,†} Sirapat Pratontep,[‡] Christian Chaumont,[§] and Jean-Claude Wittmann[†]

Institut Charles Sadron, 6, Rue Boussingault, 67083 Strasbourg, France, Ecole Européenne de Chimie des Polymères et Matériaux, 25 Rue Becquerel, 67087 Strasbourg Cedex 2, France, and National Nanotechnology Center (NANOTEC), National Science and Technology Development Agency (NSTDA), 111 Thailand Science Park, Paholyothin Road, Klong 1, Klong Luang, Patumthani 12120, Thailand

Received October 5, 2007; Revised Manuscript Received October 23, 2007

ABSTRACT: A simple method to prepare large areas of polycarbonate (PC) alignment layers with a high degree of polymer chain orientation, a periodic and oriented nanoscale pattern, and a controlled surface roughness is presented. The method involves three steps: (i) the preparation of a film of bisphenol A polycarbonate in its glassy state, (ii) the near-surface orientation of the polymer chains by rubbing, and (iii) exposure to vapors of acetone which acts as a plasticizer removing the microgrooves formed by rubbing and promotes solvent induced crystallization of PC. The resulting surface of the PC films is oriented and nanostructured, it consists of the periodic alternation of edge-on oriented crystalline lamellae and amorphous interlamellar zones with a total periodicity of ~ 20 nm. The roughness of the oriented and nanostructured PC layers can be tuned by adjusting the exposure time to the solvent. The PC films exhibit a high orienting ability for various materials grown from the vapor phase, e.g., conjugated organic semiconductors and dyes (pentacene, phthalocyanine, bisazo dye) and metallic nanoparticles. Zinc phthalocyanine nanocrystallites and gold nanoparticles are observed to orient parallel to the crystalline lamellae of the PC substrate and not, as observed for polyimides, parallel to the polymer chain direction. It is proposed that the shallow surface nanocorrugation associated with the semicrystalline structure of the PC layers enforces the orientation of the ZnPc nanocrystallites and the gold nanoparticles.

I. Introduction

A large spectrum of applications and technologically relevant objects, e.g., polarized color filters and organic field effect transistors (OFETs), involve polymer layers and surfaces showing various degrees of order and patterns at different length scales ranging from molecular to microscopic scales. Polymer surfaces with a high degree of polymer chain orientation are widely used as alignment layers in LCDs,¹ whereas nanostructured polymer films can be of interest for their optical properties, e.g., as antireflective coatings.² Numerous technologies have been developed to fabricate both oriented polymer layers and periodic polymer arrays. For instance, near-surface polymer chain alignment is readily achieved by rubbing a polymer film, typically a polyimide, with a velvet tissue.^{1,3,4} This method makes it possible to prepare large areas of alignment layers with a high orienting capacity, but the presence of microgrooves a few tens of nanometers deep prevents a good control of the surface roughness.⁵ However, this can be detrimental to certain applications, e.g., in the case of organic field effect transistors for which the structure of the interface between the organic semiconductor and the polymer gate dielectric is essential. Ideally, the polymer film used as a gate dielectric in an OFET should be pinhole free, have a large electric breakdown field, and play the role of an alignment layer to orient the organic semiconductor (pentacene for instance) in order to reach higher charge mobilities.⁶

Beside the rubbing technique, there are several other alternative methods to prepare orienting layers like for instance the friction transferred (FT) poly(tetrafluoroethylene) (PTFE) layers.⁷ Oriented PTFE films have demonstrated exceptional orienting properties for a large class of polymers and small molecules, but because of their discontinuity in terms of coverage, they are not adapted to the fabrication of oriented polymer gate dielectrics in OFETs. Other methods have also been considered for that purpose, e.g., orientation under polarized UV irradiation of liquid-crystalline polymers, a method that implies however the synthesis of specific polyimide derivatives.⁸ On the other hand, large areas of polymer surfaces showing regular oriented patterns with periodicities in the range 10–50 nm are readily prepared by using block copolymers like poly(isoprene)-*b*-poly(styrene) diblocks that form well-defined microstructures with a controlled periodicity. The periodicity and the microstructures formed in these block copolymer films can be tuned by adjusting the total length of the copolymer and the volume fraction of the two blocks, respectively.^{9,10} Nevertheless, most of the copolymers used for that purpose, e.g., poly(styrene)-*b*-poly(isoprene), are amorphous and can therefore not enforce an orientation at the molecular scale like the rubbed alignment layers.

To the best of our knowledge, there exists no simple method to prepare large areas of polymer surfaces that exhibit a high degree of polymer chain orientation, a regular and oriented pattern with a periodicity below 100 nm, and a well controlled surface roughness. Herein, we demonstrate that the combination of the preorientation of a polymer layer, prepared in its amorphous form, by a conventional rubbing method, followed by a solvent induced crystallization (SINC) allows for the

* Corresponding author. E-mail: Brinkman@ics.u-strasbg.fr.

[†] Institut Charles Sadron.

[‡] National Science and Technology Development Agency (NSTDA).

[§] Ecole Européenne de Chimie des Polymères et Matériaux.

preparation of large areas of oriented and nanostructured polymer surfaces¹¹ which indeed combine well controlled surface roughness and high orienting capacity.

II. Experimental Part

(a) Preparation of the PC Alignment Layers. Amorphous PC films of thickness in the range 200–500 nm were prepared by spin coating (2000 rpm, 500 rpm/s) a 2 wt % solution of bisphenol A polycarbonate (Acros, $M_w = 64\,000$ g/mol) in dichloromethane on clean glass slides (Corning 2947). The glass slides were cleaned by sonication in acetone and ethanol for 15 min each. Then, the slides were gently rubbed with a soft tooth brush in a 5% (by weight) solution of Hellemanex (Helma GmbH&Co., KG) in desionized water. The slides were further sonicated in a 5 wt % solution of Hellemanex for 15 min and subsequently rinsed and sonicated in desionized water for 15 min. After three rinsing steps, the slides were finally dried in a flow of nitrogen. The rubbing of the amorphous layer is performed by using a homemade apparatus. Rubbing was performed at 25 °C by using a rotating cylinder (4 cm diameter) covered with a velvet cloth applied with a pressure of 2 bar on the PC film.¹² The rubbing length was 200 cm. Exposure of the thin films to acetone vapors was performed in a closed glass vessel (volume of ~ 400 cm³) at 25 °C containing ~ 5 mL of acetone. Optical microscopy under crossed polarizers was performed using a DMR-X Leica polarizing microscope.

A screening of the effect of various solvents on the preoriented PC films has been used to find semiquantitative criteria for the choice of a suitable solvent. The affinity of a given solvent for a given polymer is quantified by means of two parameters, the solubility parameters δ_{poly} and δ_{sol} and the surface free energies γ_{poly} and γ_{sol} of the polymer and the solvent, respectively. Using the set of published data and characteristics for solvents affecting the structure of bisphenol A polycarbonate,^{13–15} we were able to establish the following two rules given by

$$|\delta_{\text{poly}} - \delta_{\text{sol}}| / [(\delta_{\text{poly}} + \delta_{\text{sol}})/2] < 0.3 \quad (1)$$

$$\gamma_{\text{sol}} < \gamma_{\text{poly}} \quad (2)$$

Equation 1 expresses the condition for an adequate chemical affinity between the polymer and the solvent whereas equation 2 gives the required conditions for a good wetting of the polymer film by a condensation layer of the solvent when exposing the film to its vapors.

(b) Preparation of Oriented Films of Conjugated Molecular Materials and Gold Nanoparticles. Molecular semiconductors and dyes (zinc phthalocyanine, pentacene, bisazo dye) as well as gold were evaporated in an Edwards Auto306 system under a base pressure of 10^{-6} mbar. Pentacene (Fluka) and zinc phthalocyanine (Kodak) were purified by entrainer sublimation. UV–vis–near IR absorption of the thin films (300–900 nm) was measured on a Shimadzu UV-2101PC spectrometer with polarized incident light and a spectral resolution of 1 nm. The film orientation with respect to the incident light was controlled by means of a goniometer: parallel orientation corresponding to the situation where the incident beam polarization is parallel to the rubbing direction. Transmission electron microscopy (TEM) was performed in bright field, dark field, and diffraction modes using a CM12 Philips microscope equipped with a MVIII CCD camera. X-ray diffraction was performed in the $(\theta, 2\theta)$ mode using a Siemens D5000 diffractometer. The thin film morphology was investigated by atomic force microscopy (AFM) with a Nanoscope III in the tapping mode using Si tips (25–50 N/m and 280–365 kHz). Visualization of the polymer film topography was performed under soft tapping conditions (drive amplitude variation below 15% with respect to the free cantilever). Image treatments, e.g., fast Fourier transforms (FFT) were performed by using AnalySIS (Soft Imaging System) software.

III. Results and Discussion

(a) Preparation Method of Oriented and Nanostructured PC Layers. The preparation process of oriented and nanostruc-

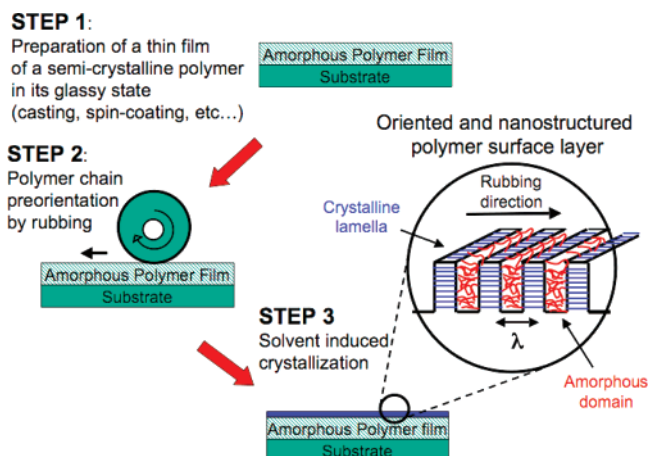


Figure 1. Schematic illustration of the various steps involved in the process used herein for the fabrication of oriented and nanostructured PC layers. The various steps are described in the text.

tured semicrystalline polymer films described hereafter is based on the periodic lamellar structure of a semicrystalline polymer as a vector to the surface nanostructuring. This process is similar to but simpler than the one described by Damman and co-workers.¹⁶ The method proposed by the latter authors involves a preorientation of a semicrystalline polymer film, prepared in its glassy state, by rubbing, followed by an annealing step (at $T \sim T_g$) to smoothen the rough morphology of the rubbed polymer surface, and finally a cold-crystallization via thermal annealing. Our process is distinct in that the smoothing of the rubbed polymer surface as well as the oriented crystallization are achieved in a single step by exposure of the preoriented polymer film to a solvent vapor which acts as a plasticizing agent and promotes solvent induced crystallization (SINC) of the polymer. In addition, the present method for the preparation of alignment layers does not require any annealing step. Accordingly, our process involves three distinct steps which are illustrated in Figure 1: (i) the preparation of a polymer film in its amorphous state either by casting or spin-coating (STEP 1 in Figure 1), (ii) near-surface alignment of the polymer chains by rubbing (STEP 2 in Figure 1), and (iii) exposure to a solvent vapor (STEP 3).

The first step of the process involves the preparation of a thin film of a semicrystalline polymer in its glassy state (STEP 1 in Figure 1). As a semicrystalline polymer we have chosen bisphenol A polycarbonate (PC). Glassy PC films are readily prepared by spin-coating a solution of the corresponding polymer in dichloromethane. In the second step of the process (STEP 2 in Figure 1), near-surface alignment of the PC chains is enforced by rubbing. The freshly rubbed PC films exhibit a uniform and very high birefringence under the polarizing optical microscope. AFM reveals a rough surface with microgrooves running parallel to the rubbing direction (see Figure 2a) and a root-mean-square (rms) roughness of typically 5 nm ($2 \times 2 \mu\text{m}^2$ area). The optical birefringence originates from both the surface orientation of the polymer chains and from the microgrooves formed by the rubbing. After the first step of rubbing, the PC films show practically no orienting ability, demonstrating that neither grapho-epitaxy nor the surface orientation of the PC chains caused by rubbing is sufficient to induce a significant orientation of molecular and inorganic materials on these surfaces.

This situation is remarkably changed when the amorphous preoriented PC films are exposed to acetone vapors (STEP 3 in Figure 1). A 2 min exposure of the rubbed polycarbonate films to acetone vapors results in a total loss of the birefringence

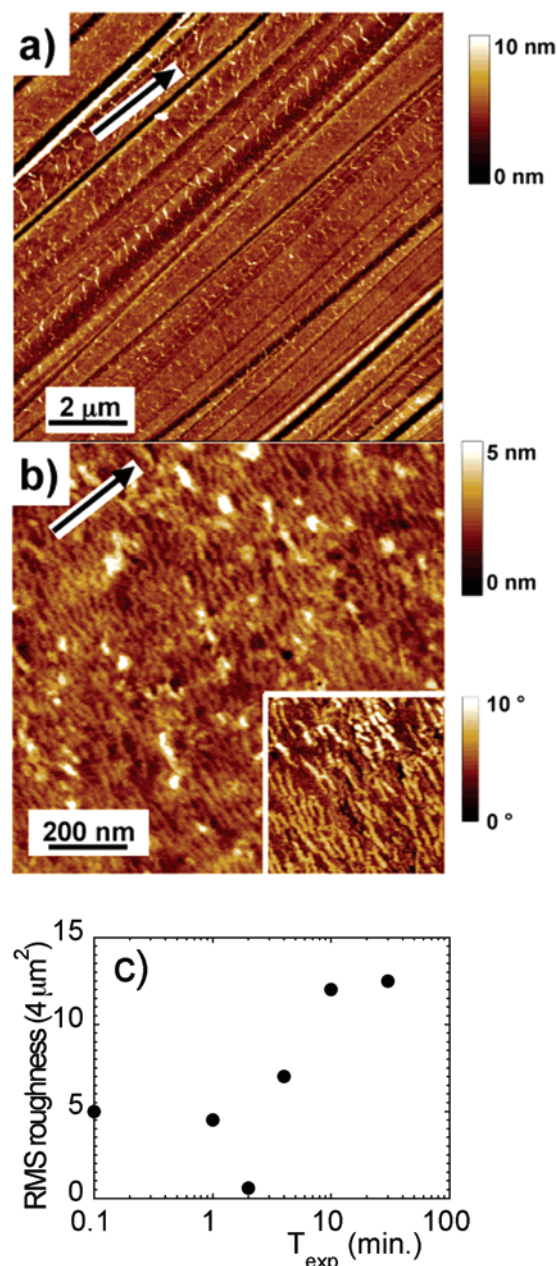


Figure 2. (a) Surface topography of a rubbed PC film (STEP 2). (b) Surface topography observed after SINC of the preoriented PC film (STEP 3). The lower right corner corresponds to the phase image. In both cases, the arrow corresponds to the rubbing direction. (c) Evolution of the surface RMS roughness of the PC films measured by AFM ($2 \times 2 \mu\text{m}^2$) as a function of the exposure time to acetone vapors.

of the films observed under the polarizing optical microscope. Furthermore, the topography of the films observed by AFM after acetone treatment does not show any trace of the microgrooves induced by the rubbing of the films (see Figure 2b). At this stage, the rms roughness of the films probed by AFM has decreased to a value of $\sim 0.5 \text{ nm}$ ($2 \times 2 \mu\text{m}^2$ area). These observations demonstrate that acetone induces a significant smoothing of the rubbed PC surface. In fact, it is well-known that acetone causes an important lowering of the glass transition temperature T_g of PC, i.e., acts as a plasticizing agent of the amorphous PC film.^{17,18} The increased plasticity of the PC films thus allows for the rough surface of the rubbed polymer films to be smoothed. However, the effect of acetone vapors is not limited to a smoothing of the rubbed PC films. As seen in Figure 2b, the topography of the PC films after 2 min exposure to

acetone vapors reveals a periodic lamellar structure. The characteristic phase contrast (see inset in Figure 2b) indicates that this morphology involves the alternation of crystalline lamellae separated by amorphous interlamellar zones. The present observation is thus clear evidence for the solvent induced crystallization of PC upon acetone vapor exposure.^{17,18} As expected, the crystalline lamellae are oriented perpendicular to the rubbing direction of the PC films, i.e., perpendicular to the oriented PC chains. The total periodicity of the lamellar structure λ measured from the fast Fourier transform (FFT) is $\sim 20 \text{ nm}$ with a very shallow surface corrugation of $\sim 1 \text{ nm}$. It is worthy to notice that the periodic nanostructuring of the polymer surface was not observed in the case of oriented poly(ethylene-terephthalate) films,¹⁶ most likely because of a partial loss of polymer chain orientation during the annealing step used to smooth the rough surface of the rubbed films.

The mechanism responsible for the oriented crystallization of PC is intimately related to the preorientation of the polymer chains by the rubbing of the films. During rubbing, bundles of PC chains are oriented parallel to the rubbing direction in a thin surface layer of the PC film and serve as a backbone for row nucleation of the oriented PC lamellae. As noticed by Kambour et al.,¹⁸ the acetone uptake by a PC film lowers significantly both the T_g and the crystallization temperature T_c , but not the melting temperature of the crystalline PC. Hence, the bundles of oriented PC chains formed during the rubbing step are preserved in the swollen and plasticized PC thin film so that they can act as oriented nuclei for the trans-crystallization of PC lamellae out of the surrounding amorphous and plasticized PC material. This crystallization process is qualified as trans-crystallization since the growth direction of the crystalline PC lamellae is perpendicular to the pre-existing bundles of oriented PC chains. To some extent, this situation reminds one of the growth of the well-known shish-kebab structure, the shish, i.e., the bundle of oriented PC chains being formed during the rubbing step (STEP 2). The present results for PC are very similar to those reported by Hobbs and Miles in the case of a shish-kebab trans-crystallization of polyethylene except that the crystallization is triggered by the exposure to a solvent vapor and not by thermal annealing.¹⁹

Increasing the exposure time T_{exp} of the films to acetone vapors above 2 min has two main consequences. First, it allows the crystallization process to proceed from the surface into the bulk of the underlying amorphous PC film. This is manifested by the emergence of a uniform birefringence of the films under the polarized light microscope. Second, it causes an increase of the surface roughness as depicted in Figure 2c. Moreover, we observe that the film surface tends to be more and more buckled with increasing T_{exp} . This surface buckling is attributed to the ongoing crystallization of PC into the bulk of the PC film.

(b) Orienting Properties of the PC Alignment Layers. We have tested the orienting ability of the smoothest nanostructured PC thin films obtained for $T_{\text{exp}} = 2 \text{ min}$ on various representative materials including various molecular semiconductors (zinc phthalocyanine (ZnPc) and acenes), organic dyes (bisazo dyes), and ordered metallic nanocluster arrays.

Figure 3 illustrates the high level of uniaxial orientation achieved for ZnPc on the oriented and nanostructured PC substrates. The ZnPc films grown at a substrate temperature $T_s = 100^\circ\text{C}$ exhibit a very regular morphology consisting of uniaxially oriented nanocrystallites. The electron diffraction (ED) pattern shown in the inset in Figure 3 is typical of the α polymorph of ZnPc with characteristic reflections at 1.18 and

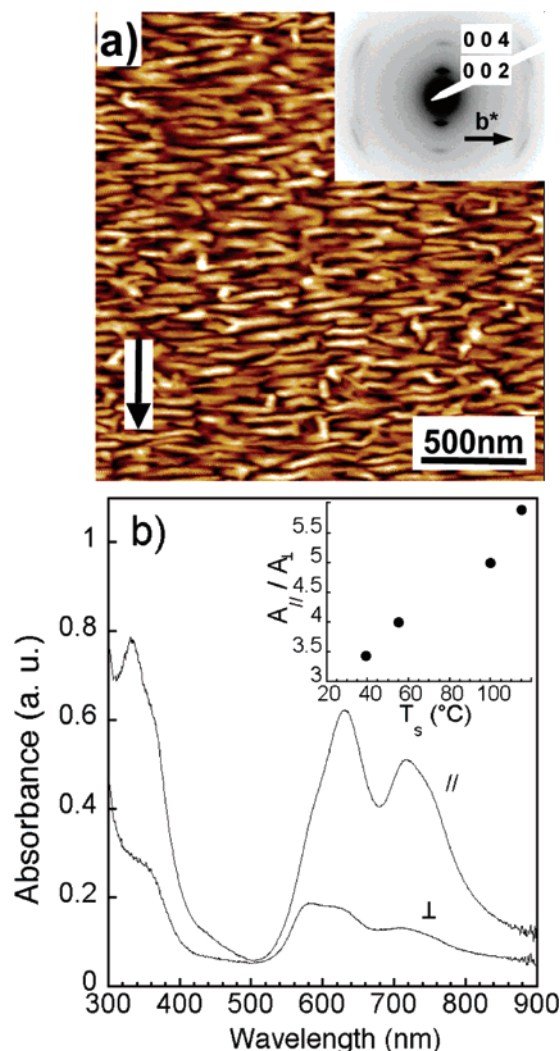


Figure 3. (a) Surface topography of an oriented ZnPc thin film (15 nm) deposited at $T_s = 100^\circ\text{C}$ on the oriented and nanostructured PC substrate. Inset: electron diffraction pattern in proper relative orientation to the morphology. The rubbing direction is indicated by an arrow. (b) Corresponding optical absorption of the oriented ZnPc film measured for parallel (\parallel) and perpendicular (\perp) orientation of the incident polarized light with respect to the rubbing direction of the PC film. The inset shows the evolution of the dichroic ratio with increasing substrate temperature T_s .

0.59 nm corresponding to the (0 0 2) and (0 0 4) planes. The sharpness of the (0 0 2) and (0 0 4) reflexions is indicative of a very high degree of unidirectional orientation in the films. The π -stacking direction of ZnPc (long axis of nanocrystals) lies perpendicular to the rubbing direction, i.e., parallel to the crystalline lamellae of the oriented PC substrate: $\mathbf{b}_{\text{ZnPc}} \perp \mathbf{c}_{\text{PC}}$. X-ray diffraction in the (θ , 2θ) mode indicates a preferential (1 0 0) contact plane of α -ZnPc on PC. Similarly to the case of PTFE substrates, the degree of orientation of ZnPc is observed to increase with increasing substrate temperature T_s .²⁰ The unidirectional orientation of α -ZnPc results in a high anisotropy of the optical absorption. Maximum absorption is observed when the polarization direction of the incident light is parallel to the PC chain direction (rubbing direction). As depicted in the inset of Figure 3b, the increase of uniaxial orientation of α -ZnPc with increasing T_s results in a corresponding increase of the dichroic ratio measured at 720 nm. For $T_s = 125^\circ\text{C}$, it reaches a value in the range 5–6 which is comparable to the values reported for oriented α -CuPc deposited onto rubbed polyimide layers.²¹

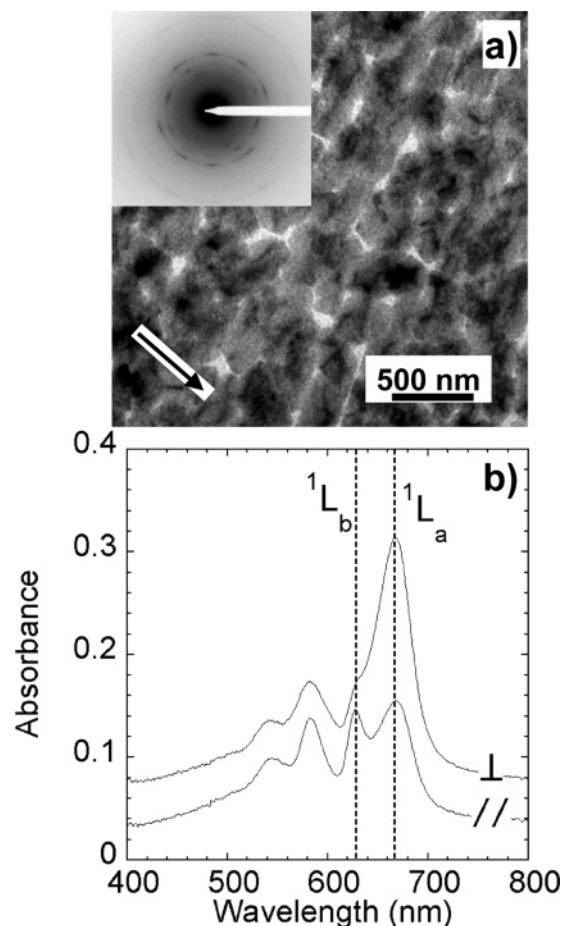


Figure 4. (a) Bright field TEM image of a 40 nm thick pentacene film deposited on oriented and nanostructured PC substrates (deposition rate = 2 nm/min). The inset corresponds to the ED pattern. The arrow in the BF image corresponds to the initial rubbing direction. (b) Polarized light absorption of the pentacene film. The spectra were shifted along the ordinate axis to clarify the whole figure.

The orienting ability of the PC layers was further tested with pentacene. In Figure 4a, we depict the typical bright field (BF) image and the corresponding ED pattern of a 40 nm thick pentacene film deposited at $T_s = 85^\circ\text{C}$ on the PC substrate. The BF image of the films shows well-defined pentacene domains with sharp edges and a preferential in-plane orientation in the direction perpendicular to the rubbing. The ED pattern shows arc-shaped reflections indicating the presence of in-plane orientation of the pentacene crystallites. The selected area electron diffraction (see Supporting Information) shows that the majority of the oriented pentacene crystals grow in the triclinic structure ($a_{\text{PEN}} = 0.606$ nm, $b_{\text{PEN}} = 0.79$ nm, $c_{\text{PEN}} = 1.49$ nm, $\alpha_{\text{PEN}} = 96.7^\circ$, $\beta_{\text{PEN}} = 100.5^\circ$, and $\gamma_{\text{PEN}} = 94.2^\circ$)²² with a (0 0 1) contact plane on the PC substrate.^{22–24} Both the observation of the oriented pentacene films under crossed polarizers (see Supporting Information) and the analysis of the ED pattern indicate that three preferred growth directions of the domains coexist on the PC substrate, but the majority of the domains grow with the \mathbf{a}_{PEN} axis perpendicular to the rubbing direction, i.e., $\mathbf{a}_{\text{PEN}} \perp \mathbf{c}_{\text{PC}}$. The in-plane orientation of pentacene domains results in the polarization of the optical absorption as seen in Figure 4b. The observed dichroic ratio of 2 for the $1L_a$ band is close to but lower than the value of 2.5–3.0 obtained for pentacene films deposited on FT PTFE.²³ The lower level of orientation of the films on PC is presently attributed to the coexistence of different orientations of the pentacene domains on the PC substrate.

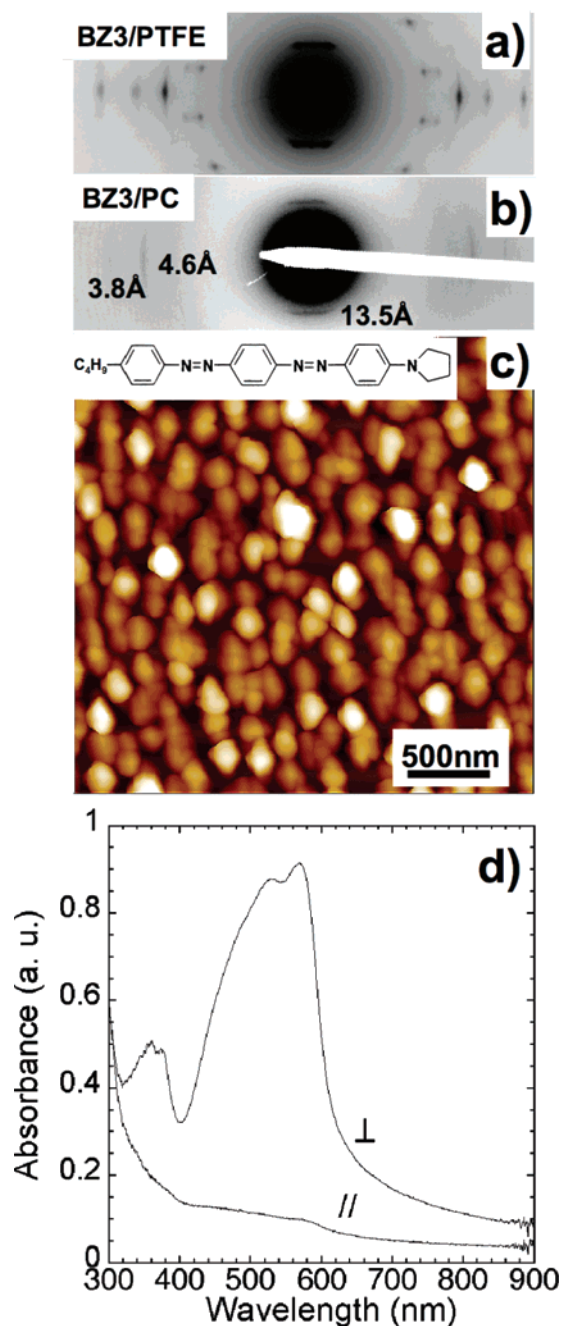


Figure 5. Typical electron diffraction pattern and morphology of a 50 nm thick bisazo dye film grown at $T_s = 29^\circ\text{C}$ on an oriented and nanostructured PC substrate. (a) ED pattern obtained for a thin film on FT PTFE, (b) ED pattern for the film deposited in the same conditions on the oriented and nanostructured PC substrate. (c) AFM topographic image. The inset depicts the chemical structure of the dye. (d) Optical absorption spectra for parallel and perpendicular orientations of the incident light with respect to the orientation of the thin films.

Significantly higher levels of orientation were observed for bisazo dyes evaporated on the PC substrates. In order to compare the orientation of the bisazo dye on the PC substrate and the FT PTFE, we show the corresponding ED patterns in Figure 5a,b. Although the ED pattern shows sharper reflections in the case of the FT PTFE substrate, a similar orientation with the same contact plane of the crystallites can be deduced from the presence of the same main reflections in the case of the PC substrate. The films deposited at $T_s = 29^\circ\text{C}$ have a dichroic ratio in the range 15–20. This value is slightly lower than that obtained in the case of thin films deposited on FT poly-(tetrafluoroethylene) substrates,²⁵ but the films grown on PC

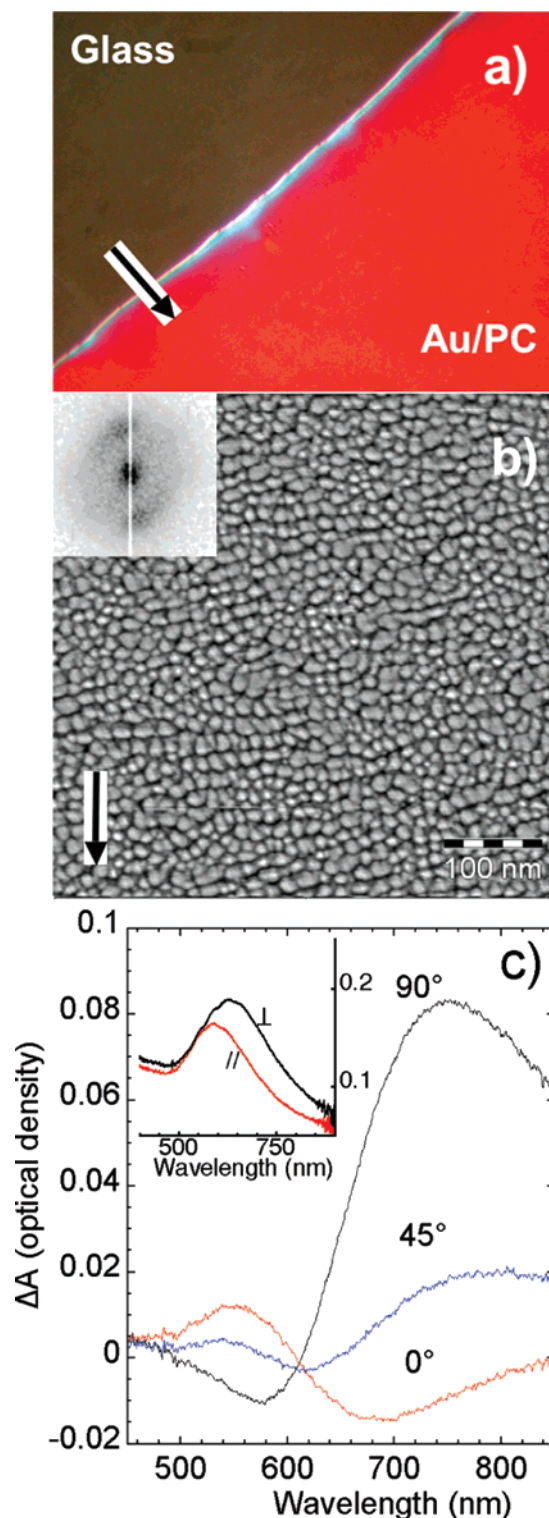


Figure 6. (a) Au/PC thin film observed by optical microscopy under crossed polarizers (45° orientation of the sample). (b) AFM image of the surface topography of Au(10 nm)/PC. The inset corresponds to the FFT. In all figures, the arrow corresponds to the rubbing direction. (c) Optical absorption spectra of Au/PC as a function of the angle between the polarization of the incident light and the rubbing direction, taking as a reference the spectrum obtained for a nonoriented Au film on PC. The inset shows the uncorrected absorption spectra of Au/PC layers.

layers are more uniform in terms of surface coverage and morphology (see Figure 5a).

Finally, the PC alignment layers were also tested for the orientation of metallic nanoparticles (see Figure 6). When observed under the polarizing microscope, the Au/PC films

behave as polarized color filters (see Figure 6a). As seen in Figure 6b, dewetting of gold on the PC surface results in the growth of oriented arrays of gold nanoparticles with a very uniform size distribution. The nanoparticles tend to align parallel to the direction of the oriented PC crystalline lamellae as observed very commonly in the case of the gold decoration technique used to reveal the lamellar structure of an oriented polymer layer.²⁶ The preferential alignment of the gold nanoparticles is also apparent from the FFT of the topographic image (see inset in Figure 6b) which shows two strong arcs in the direction parallel to the rubbing direction. The periodicity measured from the FFT corresponds to the average distance between Au nanoparticles and amounts to 17 nm which matches closely the lamellar periodicity of the nanostructured PC substrate (20 nm). These observations suggest that (i) the nanoparticles are oriented by the periodic nanocorrugation associated with the alternation of crystalline lamellae and amorphous interlamellar zones of the PC surface and (ii) the nanoparticle size is imposed by the lamellar periodicity of the PC substrate.

It is known that oriented arrays of metallic (gold, silver) nanoparticles on polymeric substrates exhibit polarized light absorption properties.²⁷ The polarized absorption of the gold films is due to the fact that the plasmon resonance frequency of the nanoparticles depends on the orientation of the polarized incident light with respect to the array of the nanoparticles.^{28,29} Figure 6c shows the dependence of the optical absorption of an oriented Au/PC film as a function of the orientation of the incident light polarization, taking as a reference the spectrum of a nonoriented gold film on a nonoriented PC substrate. Clearly, the optical absorption of the Au/PC thin films depends strongly on the angle between the incident light and the rubbing direction in the films (cf. inset in Figure 6c). Light vibrating parallel to the rubbing direction is absorbed at a lower wavelength, with a maximum at 588 nm, whereas light vibrating perpendicular to the rubbing direction shows an absorption maximum at 630 nm. The maximum of absorbance is observed when the incident polarization is perpendicular to the rubbing direction, i.e., parallel to the alignment direction of the Au nanoparticles. While yielding similar optical characteristics as those observed for FT PTFE,^{28,30} the Au/PC films show a much higher level of uniformity in terms of coverage, i.e., reduced light scattering since the PC substrates are extremely smooth in comparison to PTFE layers.

(c) Origin of the Oriented Growth. First experiments highlight the important role of the surface nanostructure on the orientation of ZnPc and Au nanoparticles on the PC layers. Figure 7 depicts the AFM phase mode image of a ZnPc film deposited through a shadow mask onto the PC substrate. In the boundary zone between covered and uncovered areas of the PC substrate, it is possible to observe both the periodic semicrystalline structure of the PC substrate and the oriented nanocrystallites of the ZnPc overlayer. From Figure 7, one can see that the ZnPc nanocrystallites grow parallel to the crystalline lamellae of the PC substrate. Similarly, Au nanoparticles are observed to align preferentially parallel to the PC lamellae and their average size matches closely the lamellar periodicity of the PC substrate. These observations suggest that the periodic nanostructuring of the PC surface, i.e., the alternation of crystalline lamellae and amorphous interlamellar zones plays a major role in the orientation of these two materials grown from the vapor phase. We suggest that the shallow nanocorrugation associated with the periodic lamellar structure of the films is sufficient to induce anisotropy in the molecular surface diffusion and hence

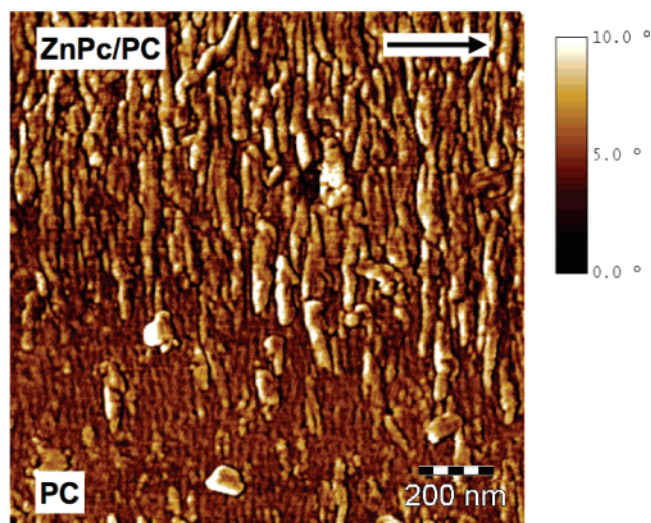


Figure 7. AFM phase-mode image of the borderline area (corresponding to the edge of a shadow mask) between the PC substrate (lower part of the image) and the ZnPc covered PC substrate (upper part). Note the alignment of the ZnPc nanocrystals parallel to the direction of the PC crystalline lamellae. The arrow in the upper right corner corresponds to the rubbing direction.

anisotropic growth of the nanocrystallites in the grooves between successive crystalline PC lamellae. This situation is similar to that observed in the case of PTFE. It has been shown that pentacene nanocrystallites grow in a confined manner between PTFE fibrils giving rise to a growth mechanism similar to grapho-epitaxy.^{23,31} However, in the case of the PC substrates, the fact that ZnPc, pentacene, and the bisazo dye grow with one preferred contact plane on the PC substrate may indicate a preferred epitaxial interaction at the overlayer/PC interface. A detailed analysis of the crystalline structure of the PC surface, using grazing incidence X-ray diffraction, is necessary in order to fully discriminate between epitaxy and grapho-epitaxy on this oriented and nanostructured surface.

IV. Conclusion

A simple and versatile method to prepare large areas of PC alignment layers with a periodic nanostructured polymer surface, oriented polymer chains, and a controlled surface roughness has been demonstrated. Among the investigated π -conjugated molecular materials (pentacene, ZnPc, bisazo dye, and coronene), the best orientation is observed for a linear rodlike bisazo dye. In addition, it has been shown that the orientation of ZnPc is improved by increasing the substrate temperature during deposition. Although the level of orientation depends strongly on the molecular system, the preparation method of PC alignment layers presented in this study has various advantages over existing fabrication routes, e.g., the rapidity of the process, the controlled roughness of the substrates, and the absence of annealing. Preliminary results indicate that the method used to prepare the alignment layers of PC can be applied to isotactic polystyrene (see Supporting Information).

In the case of phthalocyanines, it has been shown that the long axis of the elongated nanocrystallites (*b*-axis) is oriented parallel to the plane of the crystalline lamellae and not, as observed on rubbed polyimides, parallel to the polymer chains. This result suggests that the surface nanocorrugation associated with the periodic alternation of crystalline PC lamellae separated by amorphous interlamellar zones is able to induce the orientation of the ZnPc nanocrystallites. However, a detailed analysis of the crystalline structure of the PC surface, using grazing incidence X-ray diffraction, is necessary in order to fully

discriminate between epitaxy and grapho-epitaxy on this oriented and nanostructured surface.

Acknowledgment. We are grateful to Bernard Lotz and Marc Schmutz for fruitful discussions. Dr. Toshihiko Tanaka (Sumitomo Chemical Co.) is gratefully acknowledged for providing a sample of the bisazo dye. Christoph Contal is acknowledged for his valuable help in AFM. Laurent Herrmann and Gérard Strub are gratefully acknowledged for the design and fabrication of the rubbing machine. This work was supported by EEC Contract HPR-CT-2002-0327 and the Franco-Thai PHC "Nanostructured Interfaces in Electroactive Organic Architectures".

Supporting Information Available: Selected area electron diffraction (SAED) of a pentacene thin film (40 nm) deposited at $T_s = 29^\circ\text{C}$ on oriented and nanostructured PC 40 nm-thick pentacene films on PC substrates observed under crossed polarizers and showing the existence of pentacene domains with different orientations, topography of an oriented film of coronene (50 nm) grown at $T_s = 29^\circ\text{C}$ on a PC substrate, and surface topography of a thin isotactic polystyrene (iPS) thin film prepared by combining rubbing and surface crystallization. This material is available free of charge via the Internet at <http://pubs.acs.org>.

References and Notes

- (1) Depp, S. W.; Howard, W. E. *Sci. Am.* **1993**, 268, 90.
- (2) Ibn-Elhaj, M.; Schadt, M. *Nature* **2001**, 410, 796.
- (3) Geary, J. M.; Goodby, J. W.; Kmetz, A. R.; Patel, J. S. *J. Appl. Phys.* **1987**, 62, 4100.
- (4) Toney, M. F.; Russell, T. P.; Logan, J. A.; Kikuchi, H.; Sands, J. M.; Kumar, S. K. *Nature* **1995**, 374, 709.
- (5) Kim, Y. B.; Olin, H.; Park, S. Y.; Choi, J. W.; Matuszczyk, M.; Lagerwal, S. T. *Appl. Phys. Lett.* **1995**, 66, 2218.
- (6) Steudel, S.; De Vusser, S.; De Jonge, S.; Janssen, D.; Verlaak, S.; Genoe, J.; Heremans, P. *Appl. Phys. Lett.* **2004**, 85, 4400.
- (7) Wittmann, J.-C.; Smith, P. *Nature* **1991**, 352, 414.
- (8) (a) Gibbons, W. M.; Shannon, P. J.; Sun, S.-T.; Swetlin, B. J. *Nature* **1991**, 351, 49. (b) Schadt, M.; Schmitt, K.; Koznikov, V.; Chigrinov, V. *Jpn. J. Appl. Phys.* **1992**, 31, 2155. (c) Jin, S.-H.; Seo, H.-U.; Shin, W. S.; Choi, J.-H.; Yoon, U. C.; Lee, J.-W.; Song, J.-G.; Shin, D.-M.; Cal, Y.-S. *J. Mater. Chem.* **2005**, 15, 5029.
- (9) (a) Segalman, R. A.; Yokoyama, H.; Kramer, E. J. *Adv. Mater.* **2001**, 13, 1152. (b) Li, L.; Yokoyama, H. *Adv. Mater.* **2005**, 17, 1432.
- (10) Lazzari, M.; Lopez-Qunitela, M. A. *Adv. Mater.* **2003**, 15, 1583.
- (11) Brinkmann, M.; Wittmann, J.-C. PCT/FR2006/002201.
- (12) Becker, M. E.; Kilian, R. A.; Kosmowski, B. B.; Milynsky, D. A. *Mol. Cryst. Liq. Cryst.* **1986**, 132, 167.
- (13) Heiss, L. H. *Polym. Eng. Sci.* **1979**, 19, 625.
- (14) Barton, A. F. M. *Chem. Rev.* **1975**, 75, 731.
- (15) McGinniss, V. D. Vaporous Solvent Treatment of Thermoplastic Substrates. U.S. Patent 4,529,563, July 16, 1985.
- (16) (a) Damman, P.; Zolotukhin, M. G.; Villiers, D.; Geskin, V. M.; Lazzaroni, R. *Macromolecules* **2005**, 38, 2. (b) Coppée, S.; Geskin, V. M.; Lazzaroni, R.; Damman, P. *Macromolecules* **2004**, 37, 244.
- (17) Mercier, J. P.; Groeninckx, G.; Lesne, M. *J. Polym. Sci., Part C* **1967**, 16, 2059.
- (18) Kambour, R. P.; Karasz, F. E.; Daane, J. H. *J. Polym. Sci., Part A-2* **1966**, 4, 327.
- (19) Hobbs, J. K.; Miles, M. J. *Macromolecules* **2001**, 34, 353.
- (20) (a) Brinkmann, M.; Wittmann, J.-C.; Barthel, M.; Hanack, M.; Chaumont, C. *Chem. Mater.* **2002**, 14, 904. (b) Moulin, J.-F.; Brinkmann, M.; Thierry, A.; Wittmann, J.-C. *Adv. Mater.* **2002**, 14, 436.
- (21) Manaka, T.; Tagushi, K.; Ishikawa, K.; Takezoe, H. *Jpn. J. Appl. Phys.* **2000**, 39, 491.
- (22) (a) Campbell, D. J.; Robertson, J. M.; Trotter, J. *Acta Crystallogr.* **1961**, 14, 705. (b) Campbell, D. J.; Robertson, J. M.; Trotter, J. *Acta Crystallogr.* **1962**, 15, 289.
- (23) Brinkmann, M.; Graff, S.; Straupé, C.; Wittmann, J.-C.; Chaumont, C.; Nüesch, F.; Aziz, A.; Schaer, M.; Zuppiroli, L. *J. Phys. Chem. B* **2003**, 107, 10531.
- (24) Pratontep, S.; Brinkmann, M.; Nüesch, F.; Zuppiroli, L. *Synth. Met.* **2004**, 146, 387.
- (25) Tanaka, T.; Honda, Y.; Ishitobi, M. *Langmuir* **2001**, 17, 2192.
- (26) Wittmann, J.-C.; Lotz, B. *Prog. Polym. Sci.* **1990**, 15, 909.
- (27) Dirix, Y.; Bastiaansen, C.; Caseri, W.; Smith, P. *Adv. Mater.* **1999**, 11, 223.
- (28) Quinten, M.; Kreibitz, U. *Surf. Sci.* **1986**, 172, 557.
- (29) De Leon, A. G.; Dirix, Y.; Staedler, Y.; Feldman, K.; Hähner, G.; Caseri, W. R.; Smith, P. *Appl. Opt.* **2000**, 39, 4847.
- (30) Midaki, M.; Chikamastu, M.; Tanigaki, N.; Yamashita, Y.; Ueda, Y.; Yase, K. *Adv. Mater.* **2005**, 17, 297.
- (31) Givargizov, E. I. Artificial Epitaxy (Graphoepitaxy). In *Handbook of Crystal Growth*, Vol. 3; Hurler, D. T. J., Ed.; Elsevier Science: New York, 1994.

MA702227F